

# Inactivation of the Osteopontin Gene Enhances Vascular Calcification of Matrix Gla Protein-deficient Mice: Evidence for Osteopontin as an Inducible Inhibitor of Vascular Calcification In Vivo

Mei Y. Speer,<sup>1</sup> Marc D. McKee,<sup>2</sup> Robert E. Guldberg,<sup>3</sup> Lucy Liaw,<sup>4</sup>  
Hsueh-Ying Yang,<sup>1</sup> Elyse Tung,<sup>1</sup> Gerard Karsenty,<sup>5</sup>  
and Cecilia M. Giachelli<sup>1</sup>

<sup>1</sup>Bioengineering Department, University of Washington, Seattle, WA 98195

<sup>2</sup>Department of Anatomy and Cell Biology, and Faculty of Dentistry, McGill University, Montreal, Quebec, Canada H3A 2T5

<sup>3</sup>School of Mechanical Engineering, Georgia Institute of Technology, Atlanta, GA 30332

<sup>4</sup>Maine Medical Center Research Institute, Scarborough, ME 04074

<sup>5</sup>Department of Molecular and Human Genetics, Baylor College of Medicine, Houston, TX 77030

## Abstract

Osteopontin (OPN) is abundantly expressed in human calcified arteries. To examine the role of OPN in vascular calcification, OPN mutant mice were crossed with matrix Gla protein (MGP) mutant mice. Mice deficient in MGP alone (MGP<sup>-/-</sup> OPN<sup>+/+</sup>) showed calcification of their arteries as early as 2 weeks (wk) after birth ( $0.33 \pm 0.01$  mmol/g dry weight), and the expression of OPN in the calcified arteries was greatly up-regulated compared with MGP wild-types. OPN accumulated adjacent to the mineral and colocalized to surrounding cells in the calcified media. Cells synthesizing OPN lacked smooth muscle (SM) lineage markers, SM  $\alpha$ -actin and SM22 $\alpha$ . However, most of them were not macrophages. Importantly, mice deficient in both MGP and OPN had twice as much arterial calcification as MGP<sup>-/-</sup> OPN<sup>+/+</sup> at 2 wk, and over 3 times as much at 4 wk, suggesting an inhibitory effect of OPN in vascular calcification. Moreover, these mice died significantly earlier ( $4.4 \pm 0.2$  wk) than MGP<sup>-/-</sup> OPN<sup>+/+</sup> counterparts ( $6.6 \pm 1.0$  wk). The cause of death in these animals was found to be vascular rupture followed by hemorrhage, most likely due to enhanced calcification. These studies are the first to demonstrate a role for OPN as an inducible inhibitor of ectopic calcification in vivo.

Key words: biomineralization • gene knockout • phenotype transition • smooth muscle cells • vessel rupture

## Introduction

Vascular calcification is widespread in individuals with atherosclerosis, diabetes mellitus, and chronic renal failure. It occurs at two histological sites of arteries: intima, where it is commonly associated with atheromas and complicated lesions of atherosclerosis (1, 2), and media, where Mönckeberg's sclerosis forms, such as calcification of coronary artery in type I diabetic patients (2, 3). Epidemiological studies have shown that vascular calcification, determined by electron beam computed tomography, is positively correlated with atherosclerotic plaque burden and increased risk

of myocardial infarction (1, 4–6), increased ischemic episodes in peripheral vascular disease (7), and increased morbidity after angioplasty (8). Using autopsy specimens, calcification was found to be a reliable marker of plaque instability, defined as plaques that have undergone rupture (9). Moreover, in a recent study of 79 sudden cardiac death cases, both the Framingham risk index and coronary calcification were demonstrated to be predictive of future cardiovascular events (10).

Mechanisms regulating vascular calcification are currently under investigation. Morphological studies have shown that pathological calcification of blood vessels shares features with normal embryonic bone formation and bone repair. Matrix vesicles, postulated nucleation sites for the formation of apatite mineral in cartilage and perhaps bone,

Address correspondence to Cecilia M. Giachelli, Bioengineering Department, Box 351720, Bagley Hall, University of Washington, Seattle, WA 98195. Phone: 206-543-0205; Fax: 206-616-9763; E-mail: Ceci@u.washington.edu

have been detected in calcified atherosclerotic lesions (11, 12). Furthermore, proteins involved in the regulation of skeletal bone formation have also been found to be present in human atherosclerotic lesions. These proteins include osteoprotegerin and its ligand, bone sialoprotein, bone morphogenetic protein (BMP)\*-2 and BMP-4, osteocalcin, osteonectin, matrix Gla protein (MGP), and osteopontin (OPN; 13–17).

OPN is an acidic, phosphorylated glycoprotein that was first discovered in bone and is thought to be involved in the regulation of biomineralization by promoting osteoclast function through the  $\alpha_v\beta_3$  integrin and by inhibiting apatite crystal growth (18, 19). Although OPN is not present in most normal soft tissues, it is abundant at sites of ectopic calcification in human atherosclerotic lesions (20–25), diabetic arteries (26), uremic arteriolopathy (27), and in native and prosthetic valves (28–31). In calcified arteries and valves, OPN is highly localized to the surfaces of calcified deposits (32, 33). The colocalization of OPN with calcified deposits and the finding that OPN potently inhibits calcium deposition in calcifying smooth muscle cells (SMCs) in vitro (34) suggests a role for OPN in regulating vascular calcification in vivo, although OPN-deficient mice do not have a mineralization defect per se.

Because OPN is not expressed in normal blood vessels but only appears under pathological conditions, we used MGP mutant mice that spontaneously develop vascular calcification (35) as a model of vascular injury. To delineate the function of OPN in vascular calcification in vivo, we crossed OPN mutant mice with MGP mutants and examined the arteries of the double mutant mice. We found that the inactivation of the OPN gene in MGP knockout mice significantly enhanced vascular calcification, indicating that OPN may act during an adaptive response as an inducible inhibitor.

## Materials and Methods

**Generation of MGP and OPN Knockout Mice.** MGP mutant mice were generated in a C57BL/6J background as previously described (35). OPN mutant mice were generated in a 129/SvJ  $\times$  Black Swiss background (36). The hybrid OPN mutant mice were backcrossed with Black Swiss for 7 generations followed by inbreeding for >13 generations. Animals were maintained in a specific pathogen-free environment, fed standard chow and water ad libitum, and their genotypes were determined as previously described (35, 36). To generate mice deficient in both MGP and OPN (MGP<sup>-/-</sup> OPN<sup>-/-</sup>), MGP heterozygotes (MGP<sup>+/-</sup>) were crossed with OPN homozygous null mice (OPN<sup>-/-</sup>) to generate MGP and OPN heterozygotes (MGP<sup>+/-</sup> OPN<sup>+/-</sup>). These F1 mice were used as breeders to generate nine groups of mice carrying different genotypes (F2), including MGP<sup>-/-</sup> OPN<sup>+/+</sup> and MGP<sup>-/-</sup> OPN<sup>-/-</sup>. The F2 offspring were killed by giving a lethal intraperitoneal injection of nembutol (0.3 mg/g mouse) at indicated ages for necropsy. Animals used in these studies were on a

C57BL/6  $\times$  Black Swiss hybrid background. 295 mice were examined in the studies. All protocols were approved by the Animal Use Committee, University of Washington, Seattle, WA.

**Tissue Preparation and Immunohistological Analysis of Aortas of MGP  $\times$  OPN Mutant Mice.** Aortas dissected from MGP  $\times$  OPN mutant mice were fixed in methyl Carnoy's fixative (methanol/acetic acid, 3:1) for 24 h and embedded in paraffin. 5- $\mu$ m sections were used for histochemical and immunohistochemical analysis. Hematoxylin and eosin staining was used for histology. Alizarin red S (0.5%, pH 9.0; Sigma-Aldrich) and Von Kossa staining were used to detect calcification. For immunohistochemical staining, sections were first blocked with biotin and avidin blocking reagents (Vector Laboratories) and PBS containing 0.25% bovine serum albumin and 4% serum (same species as that of secondary antibody produced). Polyclonal goat anti-OPN antibody (OP199) was used to determine OPN expression (37). Monoclonal mouse anti-smooth muscle (SM)  $\alpha$ -actin antibody (1A4; Sigma-Aldrich) and polyclonal rabbit anti-SM22 $\alpha$  antibody (provided by M. Parmacek, University of Pennsylvania, Philadelphia, PA) were used to identify SMCs. Polyclonal rat anti-murine pan macrophage antibody (BM-8; Accurate Chemical & Scientific Corp.) was used to identify macrophages. After incubation at room temperature for 1 h, the sections were incubated with biotinylated secondary antibodies (Vector Laboratories) before streptavidin-conjugated peroxidase staining or fluorophore-conjugated secondary antibodies. Sections were counterstained with methyl green (2% methyl green, 2% pyronin Y; Sigma-Aldrich).

To quantitate the expression of vascular OPN and SM  $\alpha$ -actin in MGP  $\times$  OPN mutant mice, immunohistochemically stained sections were photographed at low magnification using a phase-contrast microscope equipped with an epi-differential interference contrast system and a digital camera. Positively stained areas of the whole vessel were quantitated with MetaMorph image analysis software using an identical level of color threshold. The expression of SM  $\alpha$ -actin and OPN are expressed as a percentage of the whole vessel wall and averaged from at least four sections per sample.

**Quantitative Analysis of OPN by ELISA.** Maxisorp plates (Nunc) were coated overnight at room temperature with soluble goat anti-mouse OPN antibody (AF808; R&D Systems). The plates were blocked with PBS containing 2% bovine serum albumin and 1.5% normal goat serum, and mouse sera were added to the plate. After incubation at room temperature for 2 h, AF808-bound OPN was detected with a polyclonal rabbit anti-human OPN antibody (LF123; provided by L.W. Fisher, National Institutes of Health [NIH], Bethesda, MD) before incubation with biotinylated anti-rabbit antibody and streptavidin-conjugated peroxidase staining.

**Calcium Quantification.** Tissues were lyophilized to constant weight and decalcified with 0.6 mmol/L HCl at 37°C for 24 h. Calcium released from the lyophilized tissues was determined colorimetrically by the o-cresolphthalein complex one method as previously described (calcium diagnostic kit; Sigma-Aldrich; reference 38). The amount of vascular calcium was normalized to the dry weight of the tissues and expressed as millimolar/gram dry weight.

**High Resolution X-ray Microcomputed Tomography.** Isolated aortas from MGP  $\times$  OPN mutant mice were scanned nondestructively on a microcomputed tomography system ( $\mu$ CT 40; Scanco Medical) at a voxel resolution of 16 microns. Reconstructed image slices were stacked to create 3D images of calcified regions within the aortas. The average thickness of the calcified

\*Abbreviations used in this paper: BMP, bone morphogenetic protein; MGP, matrix Gla protein; OPN, osteopontin; SM, smooth muscle; SMC, smooth muscle cell.

region within the aortic wall was measured using direct 3D morphometric analysis (39).

**Statistical Analysis.** Data, shown as means  $\pm$  SEM, were analyzed with Student's *t* test or analysis of variance to determine the significance of differences. The association of two variables, shown as correlation coefficient, was considered statistically significant at a *P* value of  $<0.05$ . The differences between observed data and expected data were analyzed by  $\chi^2$  test and considered to be statistically significant at a *P* value of  $<0.05$ .

## Results

**Crossing of MGP Mutant Mice with OPN Mutant Mice.** As reported previously (35), MGP null homozygotes showed ectopic arterial calcification (which led to vessel rupture), cartilage calcification (which led to short stature), osteopenia, and fracture. MGP heterozygotes showed no ectopic calcification. OPN null homozygotes and heterozygotes developed normally and were grossly normal at birth, with no overt evidence of bone or vascular defects under normal conditions (16, 36).

To examine whether endogenous OPN might be involved in vascular calcification under conditions of MGP deficiency, we crossed MGP mutant mice with OPN mutant mice, as described in Materials and Methods. Analysis of 295 F2 mice showed that the frequency of nine different genotypes was close to the expected Mendelian ratio ( $\chi^2 = 4.58$ ,  $P > 0.250$ ), indicating no embryological lethality. However, mice carrying genotypes of MGP<sup>-/-</sup> OPN<sup>-/-</sup>, MGP<sup>-/-</sup> OPN<sup>+/-</sup>, MGP<sup>-/-</sup> OPN<sup>+/+</sup>, and MGP<sup>+/-</sup> OPN<sup>-/-</sup> started to die during weeks 3 and 4 after birth. By analyzing the average death ages of mice of different genotypes, a profound effect of OPN on the postnatal survival of MGP<sup>-/-</sup> mice was observed. Mice deficient in both MGP and OPN had an average death age of  $4.4 \pm 0.2$  wk, whereas MGP null mice with a wild-type OPN gene had an average death age of  $6.6 \pm 1.0$  wk ( $n = 5 - 9$ /genotype,  $P < 0.05$ ). Similar to the MGP<sup>-/-</sup> mice, vascular rupture followed by hemorrhage most likely due to severe vascular calcification, was found to be the cause of death in these animals.

**OPN Is an Inducible Inhibitor of Vascular Calcification in MGP Mutant Mice.** The expression of OPN in vessels from MGP  $\times$  OPN mutant mice was determined immunohistochemically. As shown in Fig. 1, OPN was abundant in calcified vessels of MGP<sup>-/-</sup> OPN<sup>+/+</sup> mice, but not in MGP<sup>+/+</sup> OPN<sup>+/+</sup> and MGP<sup>-/-</sup> OPN<sup>-/-</sup> arteries (A). At a higher magnification (Fig. 1, B and C), OPN was found coating mineral deposits (arrows) and it also colocalized to some cells of the calcifying medial layer (arrowheads). Quantitative analysis of the immunohistochemical images showed an age-dependent increase of OPN expression in MGP<sup>-/-</sup> OPN<sup>+/+</sup> mice (Fig. 1 D). In addition, serum OPN was determined by ELISA and was found to be increased, to a smaller degree, in MGP<sup>-/-</sup> OPN<sup>+/+</sup> mice compared with wild-types ( $1.5 \pm 0.14$   $\mu\text{g/ml}$  vs.  $1.0 \pm 0.04$   $\mu\text{g/ml}$ ;  $n = 3 - 7$ ,  $P < 0.01$ ), but completely absent in MGP<sup>-/-</sup> OPN<sup>-/-</sup> mice.

To determine the effect of OPN on arterial calcification, we examined aortas and carotid arteries from MGP  $\times$  OPN mutant mice. As shown in Fig. 2, aortas from mice deficient in MGP alone were calcified as early as 2 wk after birth and calcification increased with age. Interestingly, aortas from mice deficient in both MGP and OPN had almost twice as much calcification as MGP<sup>-/-</sup> OPN<sup>+/+</sup> at 2 wk ( $0.61 \pm 0.06$  mmol/g dry weight vs.  $0.33 \pm 0.01$  mmol/g dry weight) and over three times as much at 4 wk ( $2.02 \pm 0.07$  mmol/g dry weight vs.  $0.62 \pm 0.06$  mmol/g dry weight). Moreover,  $\sim 30\%$  of MGP<sup>+/-</sup> OPN<sup>-/-</sup> mice (8 out of 25) showed overt vascular calcification at 4–8 wk, whereas MGP<sup>+/-</sup> OPN<sup>+/+</sup> mice never showed vascular calcification at any time point observed.

As shown in Fig. 3, calcification of arteries from MGP  $\times$  OPN mutant mice was visualized in cross sections by Alizarin red S (A, red, asterisks) and Von Kossa (B, dark brown, asterisks), and in a 3D reconstruction of a segment of aorta by microcomputed tomography (C, gray, asterisks). A similar overall morphology of arterial calcification was observed in all calcifying genotypes. Calcification was mainly located in the arterial media and in the early stages was associated with elastic lamina (Fig. 3 D, asterisks). As the process proceeds, fully mineralized media, mild to moderate intimal and medial thickening (Fig. 3 A–C and E, asterisks), fragmentation of elastic laminae (G, arrows vs. normal elastic laminae in F), partially dissected arterial wall and rupture (H, arrowheads), and aneurysm formation (I, arrowheads) were observed in the calcified vessels. Taken together, these results demonstrate that the inactivation of the OPN gene enhances the magnitude of vascular calcification of MGP-deficient mice, probably leading to the accelerated mortality. These studies are the first to validate a role for OPN as an inducible inhibitor in vascular calcification in vivo.

**Correlation of Vascular Calcification with Loss of SM Lineage Markers in MGP  $\times$  OPN Mutant Mice.** We have previously reported a novel association of vascular calcification with SMC phenotypic transition, i.e., up-regulation of Cbfa1 and down-regulation of SM lineage markers (40). In this study of MGP  $\times$  OPN mutant mice, we were able to analyze this association in greater detail. As shown in Fig. 4, arteries from wild-type animals showed no calcification (A) and were strongly stained for SM lineage marker, SM  $\alpha$ -actin (D), as expected. When the arteries were partially calcified, as shown in 2-wk-old MGP<sup>-/-</sup> OPN<sup>+/+</sup> mice (Fig. 4 B), vascular  $\alpha$ -actin was retained only in the areas that had not yet undergone calcification, but not in the calcified areas (E). When the arteries were extensively calcified (Fig. 4 C), a complete loss of SM  $\alpha$ -actin expression was observed (F). Statistical analysis of 38 mice for the relationship of genotype, SM  $\alpha$ -actin expression, and vascular calcification showed that SM  $\alpha$ -actin expression was negatively correlated with calcium amount of the vessels (Fig. 4 G,  $r = -0.5200$ ,  $P < 0.001$ ), but not with genotypes (unpublished data). Similar results were obtained when aortic sections were stained for SM22 $\alpha$ , a second SM-specific marker (unpublished data). The loss of SM  $\alpha$ -actin and SM22 $\alpha$  expression in calcified arteries of MGP  $\times$  OPN mutant mice is not due to cellular

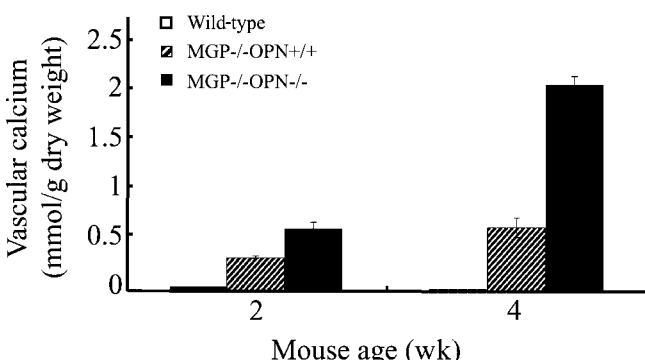
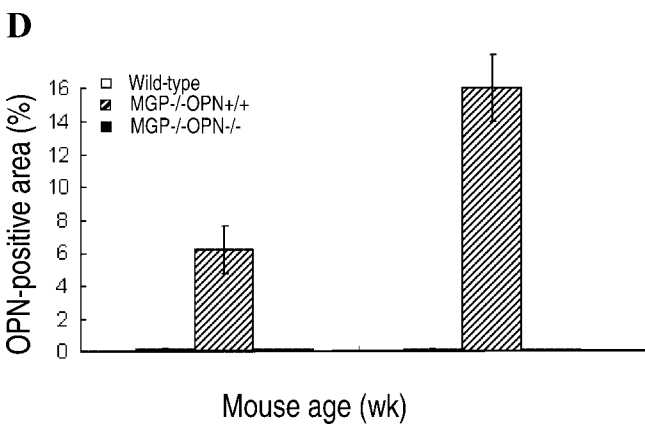
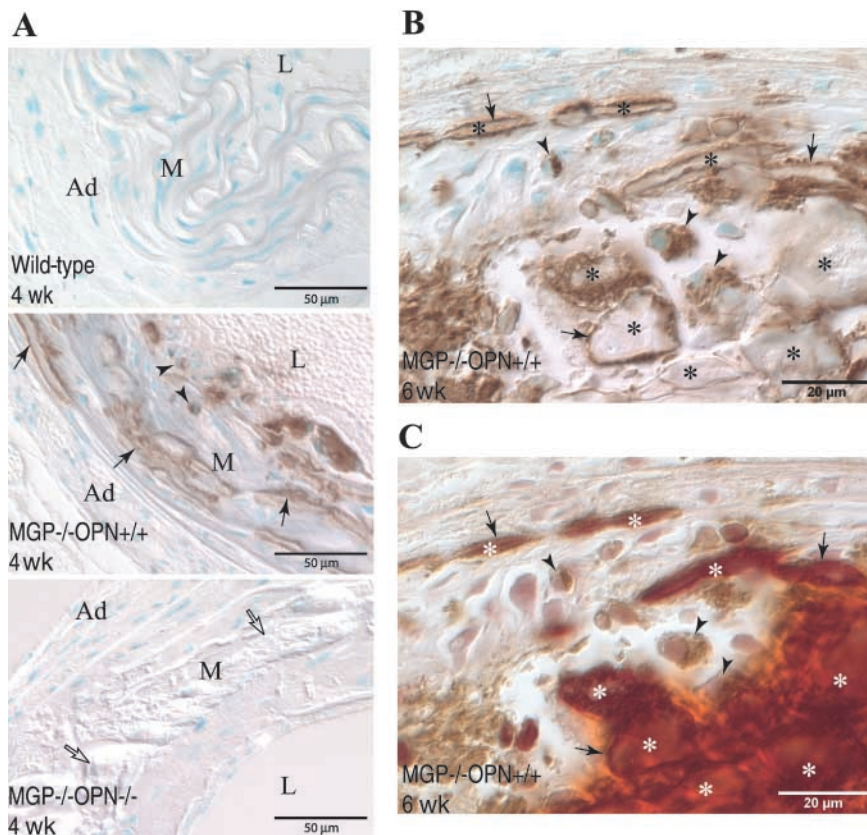


**Figure 1.** OPN expression in the calcified aortas of MGP × OPN mutant mice. (A) Aortas of 2-wk-old MGP<sup>-/-</sup> OPN<sup>+/+</sup> and MGP<sup>-/-</sup> OPN<sup>-/-</sup> mice, and their wild-type counterparts were examined immunohistochemically for OPN expression. Arrows and arrowheads indicate OPN expressed in the arterial wall. Open arrows indicate mineral deposition in the MGP<sup>-/-</sup> OPN<sup>-/-</sup> aortas, as determined by Alizarin red S staining of adjacent section (not depicted). (B and C) Double staining of aorta of a 6-wk-old MGP<sup>-/-</sup> OPN<sup>+/+</sup> mouse by immunohistochemistry for (B) OPN expression and by (C) Alizarin red S for mineral deposition. Note the association of OPN with mineral (arrows) and cells in the mineralized area (arrowheads). L, lumen; M, media; Ad, adventitia; \*, mineral. (D) OPN expression in aortas of mice carrying different genotypes was quantified by MetaMorph image analysis as described in Materials and Methods. Data shown are mean ± SEM, *n* = 4 – 10.

deficiency, as counterstaining of the sections with methyl green (Fig. 4 B, C, E, and F) and adjacent sections stained with hematoxylin and eosin (unpublished data) showed numerous nuclei in the calcified area. Moreover, cells positively stained for SM lineage markers were observed in noncalcified areas (Fig. 4 E, arrowheads) and in the small adventitial vessels of extensively calcified arteries (F, arrowheads).

**Figure 2.** Quantification of calcium amount in vessels of MGP<sup>-/-</sup> OPN<sup>+/+</sup> and MGP<sup>-/-</sup> OPN<sup>-/-</sup> mice. 2- and 4-wk-old mice with indicated genotypes were killed by nembtal and their aortas were dissected and lyophilized. Calcium content of the lyophilized vessels was determined using a Sigma-Aldrich calcium diagnostic kit as described in Materials and Methods. Data shown are mean ± SEM, *n* = 4 – 9, *F* = 106.5, *P* < 0.0001 (analysis of variance).

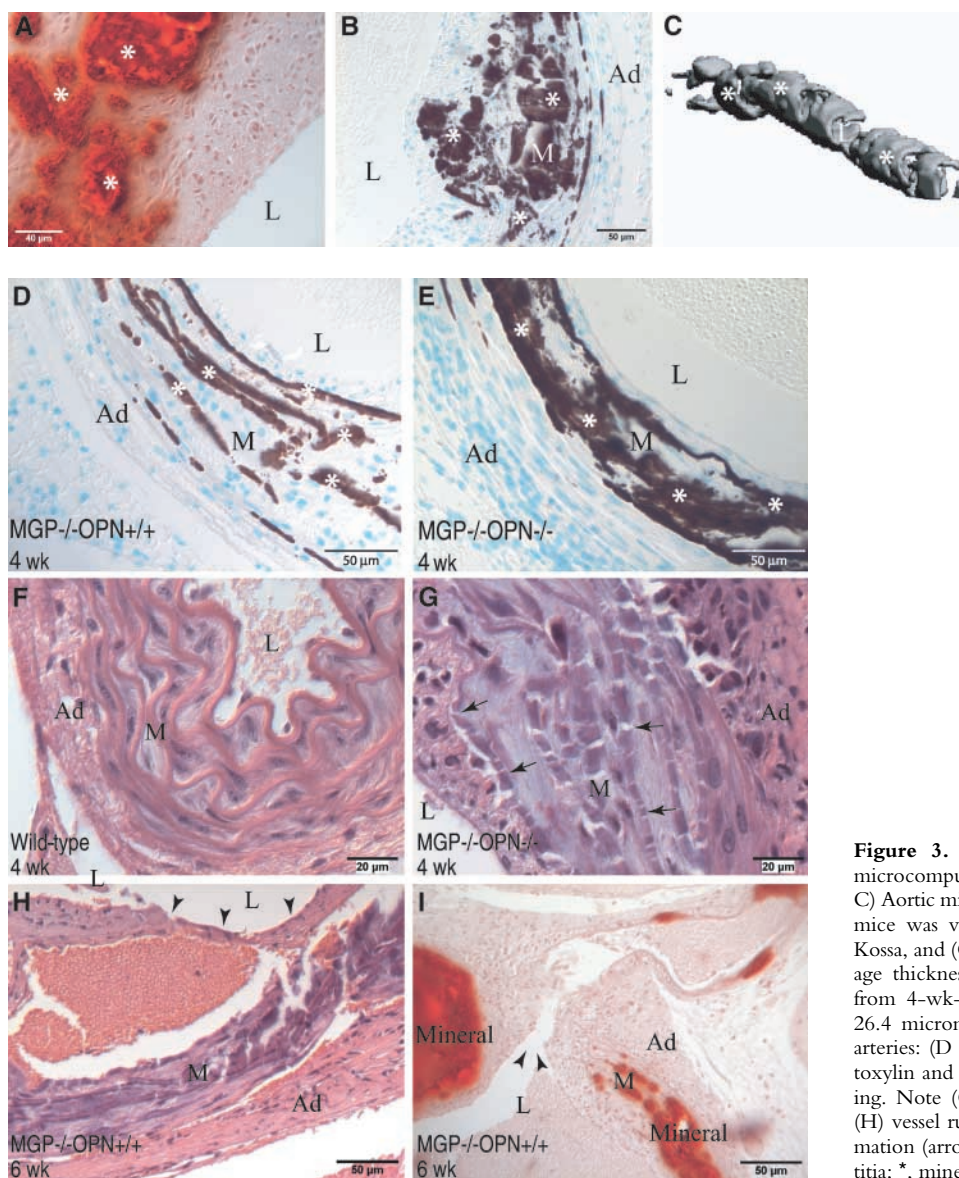


**Figure 3.** Representative histological analyses and microcomputed tomography of calcified arteries. (A–C) Aortic mineralization of 4-wk-old  $MGP^{-/-} OPN^{+/-}$  mice was visualized by (A) Alizarin red S, (B) Von Kossa, and (C) microcomputed tomography. The average thickness of the calcified region for three aortas from 4-wk-old  $MGP^{-/-} OPN^{+/-}$  mice was  $92.2 \pm 26.4$  microns. (D–I) Histological analyses of calcified arteries: (D and E) Von Kossa staining, (F–H) Hematoxylin and eosin staining, and (I) Alizarin red S staining. Note (G) elastic laminae fragmentation (arrows), (H) vessel rupture (arrowheads), and (I) aneurysm formation (arrowheads). L, lumen; M, media; Ad, adventitia; \*, mineral.

*Vascular Cells, But Not Macrophages, Are the Predominant Cells Synthesizing OPN.* As shown in Fig. 1 B, cells in the calcifying medial layer of MGP mutant mice synthesized OPN. To further characterize these cells, arteries dissected from MGP mutant mice were stained immunohistochemically for SMCs, the predominant cells of the arterial wall, and macrophages, the inflammatory cells reported to be present in human calcified vessels and synthesize OPN (22). As we have shown in Fig. 4 and in the previous report (40), SMCs in the calcified area lost their lineage marker, SM  $\alpha$ -actin and SM22 $\alpha$ , and gained expression of OPN. To determine whether these cells were macrophages, antibodies to BM8, a macrophage-specific surface marker, were used in immunohistochemistry. As shown in Fig. 5, there were no macrophages present in normal arteries of wild-type animals (A). However, at 2 wk, when arteries were slightly calcified (Fig. 5 C), immunostained macrophages appeared exclusively in the adventitial layer (B, arrows). At 4 wk, when

calcification was widespread, some macrophages infiltrated into the media surrounding calcium deposits (unpublished data). Using double immunohistochemical staining (Fig. 5, D–F), although macrophages were found to synthesize OPN (arrows), the predominant cells expressing OPN in the calcified arteries were found in the medial layer where macrophages were absent (open arrows). Taken together, these data indicate that the major source of OPN in the calcified arteries of MGP mutant mice are vascular medial cells, most likely SMCs that had undergone phenotypic transition and some macrophages that had infiltrated into the media.

## Discussion

OPN is highly expressed in the calcified lesions of human primary and restenotic atherosclerosis (20, 22, 41), diabetes (26), and chronic renal failure (27) although little is

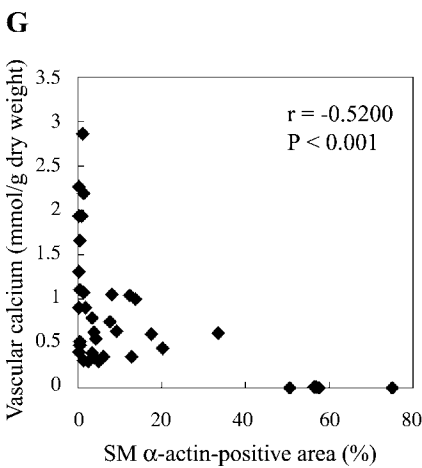
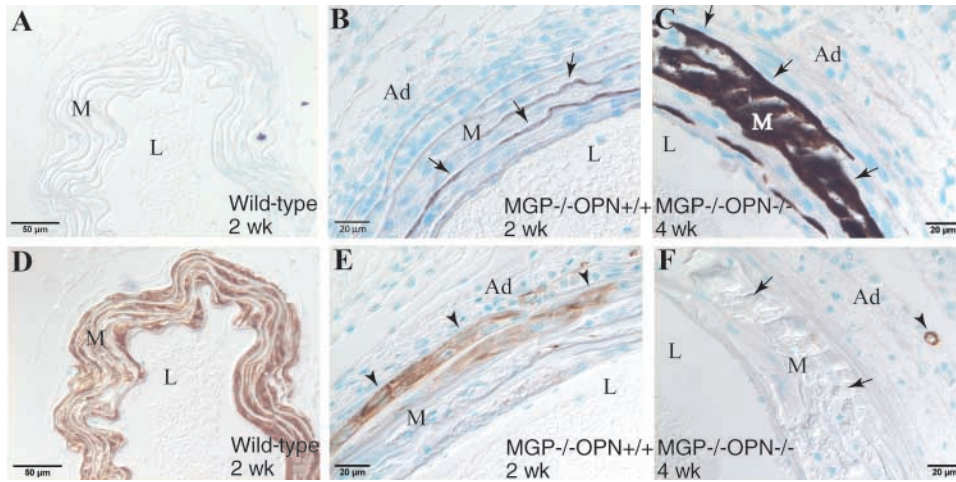


**Figure 4.** SMCs in calcified arteries lose their lineage marker, SM  $\alpha$ -actin. (A–C) Aortas of 2- and 4-wk-old MGP  $\times$  OPN mutant mice were examined for mineral deposition by Von Kossa staining (arrows) and (D–F) for SM  $\alpha$ -actin by immunohistochemistry (arrowheads). Note the loss of SM  $\alpha$ -actin in the mineralized area of aortas from (E) 2-wk and (F) 4-wk MGP<sup>-/-</sup> OPN<sup>-/-</sup> mice. L, lumen; M, media; Ad, adventitia. (G) Correlation of aortic SM  $\alpha$ -actin expression and calcium deposition. SM  $\alpha$ -actin expression in the aortas of MGP  $\times$  OPN mutant mice was quantified by MetaMorph image analysis of the stained sections and the corresponding vascular calcium deposition by determining the acid-released calcium using a Sigma-Aldrich calcium diagnostic kit as described in Materials and Methods.  $n = 38$ ,  $P < 0.001$ .

known about its role in these lesions. In this study, we have demonstrated for the first time the inhibitory effect of OPN on vascular calcification in vivo. Using MGP mutant mice as a vascular calcification model, endogenous OPN

expression was found to be dramatically up-regulated in cells of the arterial media where ectopic mineralization had formed. Concomitant with the gain of OPN expression, the expression of SM lineage markers, SM  $\alpha$ -actin and

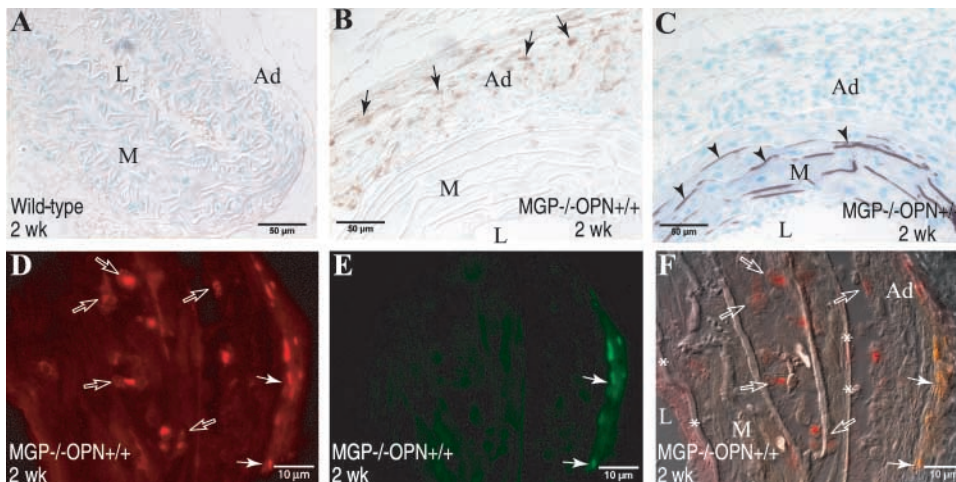


**Figure 5.** Macrophages are not the predominant cells to synthesize OPN in calcified aortas of MGP  $\times$  OPN mutant mice. (A and B) Aortas of 2-wk-old MGP  $\times$  OPN mutant mice were stained immunohistochemically for macrophages using streptavidin-conjugated peroxidase. Note the recruitment of macrophages into (B) adventitia of calcified arteries (arrows), but not in (A) normal vessels. (C) Adjacent section stained for mineral (arrowheads) by Von Kossa. Colocalization of macrophages and OPN was further determined by double immunohistochemical staining using fluorophore-conjugated secondary antibodies. (D) Rhodamine-OPN, (E) Cyanine-BM8, and (F) Overlay

of D and E onto a differential interference contrast photo of the same field. Note OPN<sup>+</sup> cells (red in D and red and yellow in F) were present mostly in the medial layer where macrophages (green in E and green and yellow in F) were absent. Arrows, macrophages; open arrows, OPN-expressing cells except macrophages; arrowheads, mineral; L, lumen; M, media; Ad, adventitia; \*, internal and external elastic laminae.

SM22 $\alpha$ , declined substantially in calcified arteries. Cells synthesizing OPN were found to be mainly vascular medial cells, most likely SMCs that had undergone phenotypic transition and in a lower percentage, infiltrated macrophages. Furthermore, in comparison with mice deficient in MGP alone (MGP<sup>-/-</sup> OPN<sup>+/+</sup>), mice lacking both MGP and OPN (MGP<sup>-/-</sup> OPN<sup>-/-</sup>) showed accelerated and enhanced medial calcification. The enhanced calcification correlated with decreased survival of the mice, most likely due to increased vessel rupture and hemorrhage. Finally, although MGP<sup>+/-</sup> OPN<sup>+/+</sup> mice never showed calcification, ~30% of MGP<sup>+/-</sup> OPN<sup>-/-</sup> mice had calcified arteries. Taken together, these observations demonstrate for the first time an adaptive mechanism by which OPN serves as an important inducible mediator to inhibit vascular calcification in vivo.

Vascular calcification is an actively regulated process that may involve chondrogenic and/or osteogenic differentiation of vascular cells and the expression of bone-related mediators and inhibitors. Support for the concept of active regulation of vascular calcification is best exemplified by the occurrence of vascular calcification in the MGP null mouse. MGP is a small matrix protein originally found in developing bone (42). It contains several  $\gamma$ -carboxyglutamic acid residues (Gla residues), most of which are clustered centrally in the protein, providing a negatively charged region for the protein to bind to hydroxyapatite (42–44). In normal blood vessels, the protein is secreted by SMCs and binds to elastic laminae of the tunica media and the extracellular matrix of the adventitia, and in calcified vessels, the protein accumulates at the interface between mineralized and nonmineralized areas (45, 46).

Although the mechanism by which MGP inhibits vascular calcification is not yet known, several possibilities have been posited. First, MGP may act as a calcification “surveillance” inhibitor by binding to small calcium phosphate precipitates and removing them via the circulation, thus preventing the vessels from becoming mineralized (47–49). In support of this, rats treated with the bisphosphonate etidronate, showed elevated serum levels of a protein–mineral complex consisting of calcium, phosphate, fetuin, and MGP (47). Alternatively, MGP may normally prevent inappropriate differentiation within the blood vessel because it was recently reported to be an inhibitor of BMP-2, a factor promoting osteogenic and chondrogenic differentiation (50). Finally, MGP may inhibit vascular calcification via direct interaction with putative nucleating sites in the elastic lamina, as these structures are the preferred sites for initiation of mineral deposition in the MGP null mouse as well as in warfarin-treated rats and Mönckeberg’s medial sclerosis (35, 45, 51, 52).

OPN, on the other hand, is not constitutively expressed in blood vessels, but rather is induced by various injurious stimuli (32). Indeed, OPN was only expressed in calcified vessels of the MGP mutant mice. Thus, OPN appears to function as an inducible “damage control” inhibitor of calcification. The mechanism by which OPN inhibits miner-

alization is also unclear, but physical inhibition of apatite deposition and accumulation is likely. OPN has a high content of aspartic acid residues and is highly phosphorylated on serine and threonine residues. This structure enables OPN to bind to hydroxyapatite and calcium ions, and thus to physically inhibit crystal formation and growth in vitro (19, 53, 54). Consistent with these in vitro findings, the OPN localized in the calcified arteries of MGP<sup>-/-</sup> mice in this study was found to be closely associated with mineral, predominantly accumulating on the mineral surface as a dense planar coating (Fig. 1 B) and therefore potentially acting locally to inhibit mineral growth via a direct physical interaction. Because the OPN null mice do not show vascular calcification, it is unlikely that OPN generally regulates SMC phenotype. However, we cannot rule out the possibility that lack of OPN, in the context of MGP deficiency, effects the differentiation and subsequent mineralization potential of vascular SMCs, as discussed below.

We and others have previously shown that cultured human and bovine medial SMCs have the ability to mineralize their matrices under defined culture conditions (34, 38, 55). The calcifying SMCs were further characterized to have undergone phenotypic transition to Cbfa1<sup>+</sup>, osteochondroprogenitor-like cells (40). These cells lost their SM lineage markers but gained Cbfa-1 expression, a factor required for osteogenesis and chondrocyte hypertrophy, and expressed genes containing the Cbfa1 binding site OSE2, including OPN, osteocalcin, and alkaline phosphatase (40, 46, 55–57). Moreover, the addition of exogenous OPN to cultured calcifying SMCs inhibited their ability to calcify the matrices in a dose-dependent manner (34). The ability of OPN to inhibit calcification of SMC cultures was later found to depend entirely on a posttranslational modification, phosphorylation of the protein (54).

In this study, vascular SMCs in the mineralized area of MGP-deficient mice were also found to have lost their lineage markers SM  $\alpha$ -actin and SM22 $\alpha$ , and the cells in the calcified areas, most likely phenotypically modified SMCs, were found to produce OPN. Thus, vessels undergoing mineralization appear to adapt the loss of MGP by up-regulating a potent inhibitor of mineralization, namely OPN. Furthermore, the ability to up-regulate OPN extends a survival advantage to mice. Whether endogenously produced OPN inhibits vascular calcification of MGP mutant mice via direct physical inhibition or a decrease in the mineralizing potential of medial SMCs is currently under investigation.

We thank Ms. Lynn Kemper for the maintenance of MGP and OPN mutant mice, and Dr. Kip Hauch for his assistance in using the UWEB Optical Microscopy and Image Analysis Shared Resource, funded by the National Science Foundation through grants EEC-9872882 and EEC-9529161.

This work was supported by NIH grant AR48798-01 to C.M. Giachelli and NIH training grant HL07828-06 to M.Y. Speer.

Submitted: 4 June 2002

Revised: 8 August 2002

Accepted: 21 August 2002

## References

1. Rumberger, J.A., D.B. Simons, L.A. Fitzpatrick, P.F. Sheedy, and R.S. Schwartz. 1995. Coronary artery calcium area by electron-beam computed tomography and coronary atherosclerotic plaque area. A histopathologic correlative study. *Circulation*. 92:2157–2162.
2. Lehto, S., L. Niskanen, M. Suhonen, T. Ronnema, and M. Laakso. 1996. Medial artery calcification. A neglected harbinger of cardiovascular complications in non-insulin-dependent diabetes mellitus. *Arterioscler. Thromb. Vasc. Biol.* 16:978–983.
3. Olson, J.C., D. Edmundowicz, D.J. Becker, L.H. Kuller, and T.J. Orchard. 2000. Coronary calcium in adults with type 1 diabetes: a stronger correlate of clinical coronary artery disease in men than in women. *Diabetes*. 49:1571–1578.
4. Sangiorgi, G., J.A. Rumberger, A. Severson, W.D. Edwards, J. Gregoire, L.A. Fitzpatrick, and R.S. Schwartz. 1998. Arterial calcification and not lumen stenosis is highly correlated with atherosclerotic plaque burden in humans: a histologic study of 723 coronary artery segments using nondecalcifying methodology. *J. Am. Coll. Cardiol.* 31:126–133.
5. Beadenkopf, W.G., A.S. Daoud, and B.M. Love. 1964. Calcification in the coronary arteries and its relationship to arteriosclerosis and myocardial infarction. *Am. J. Roentgenol.* 92: 865–871.
6. Puentes, G., R. Detrano, W. Tang, N. Wong, W. French, K. Narahara, B. Burndage, and H. Baksheshi. 1995. Estimation of coronary calcium mass using electron beam computed tomography: a promising approach for predicting coronary events? *Circulation*. 92:1313.
7. Niskanen, L.K., M. Suhonen, O. Siitonen, J.M. Lehtinen, and M.I. Uusitupa. 1990. Aortic and lower limb artery calcification in type 2 (non-insulin-dependent) diabetic patients and non-diabetic control subjects. A five year follow-up study. *Atherosclerosis*. 84:61–71.
8. Fitzgerald, P.J., T.A. Ports, and P.G. Yock. 1992. Contribution of localized calcium deposits to dissection after angioplasty. An observational study using intravascular ultrasound. *Circulation*. 86:64–70.
9. Burke, A.P., A. Taylor, A. Farb, G.T. Malcom, and R. Virmani. 2000. Coronary calcification: insights from sudden coronary death victims. *Z. Kardiol.* 89:49–53.
10. Taylor, A.J., A.P. Burke, P.G. O'Malley, A. Farb, G.T. Malcom, J. Smialek, and R. Virmani. 2000. A comparison of the Framingham risk index, coronary artery calcification, and culprit plaque morphology in sudden cardiac death. *Circulation*. 101:1243–1248.
11. Kim, K.M. 1976. Calcification of matrix vesicles in human aortic valve and aortic media. *Fed. Proc.* 35:156–162.
12. Tanimura, A., D.H. McGregor, and H.C. Anderson. 1986. Calcification in atherosclerosis. I. Human studies. *J. Exp. Pathol.* 2:261–273.
13. Bini, A., K.G. Mann, B.J. Kudryk, and F.J. Schoen. 1999. Noncollagenous bone matrix proteins, calcification, and thrombosis in carotid artery atherosclerosis. *Arterioscler. Thromb. Vasc. Biol.* 19:1852–1861.
14. Dhore, C.R., J.P. Cleutjens, E. Lutgens, K.B. Cleutjens, P.P. Geusens, P.J. Kitslaar, J.H. Tordoir, H.M. Spronk, C. Vermeer, and M.J. Daemen. 2001. Differential expression of bone matrix regulatory proteins in human atherosclerotic plaques. *Arterioscler. Thromb. Vasc. Biol.* 21:1998–2003.
15. Farzaneh-Far, A., D. Proudfoot, C. Shanahan, and P.L. Weissberg. 2001. Vascular and valvar calcification: recent advances. *Heart*. 85:13–17.
16. Rittling, S.R., H.N. Matsumoto, M.D. McKee, A. Nanci, X.R. An, K.E. Novick, A.J. Kowalski, M. Noda, and D.T. Denhardt. 1998. Mice lacking osteopontin show normal development and bone structure but display altered osteoclast formation in vitro. *J. Bone Miner. Res.* 13:1101–1111.
17. Asou, Y., S. Rittling, H. Yoshitake, K. Tsuji, K. Shinomiya, A. Nifuji, D. Denhardt, and M. Noda. 2001. Osteopontin facilitates angiogenesis, accumulation of osteoclasts, and resorption in ectopic bone. *Endocrinology*. 142:1325–1332.
18. Denhardt, D.T., and X. Guo. 1993. Osteopontin: a protein with diverse functions. *FASEB J.* 7:1475–1482.
19. Boskey, A.L., M. Maresca, W. Ullrich, S.B. Doty, W.T. Butler, and C.W. Prince. 1993. Osteopontin-hydroxyapatite interactions in vitro: inhibition of hydroxyapatite formation and growth in a gelatin-gel. *Bone Miner.* 22:147–159.
20. Giachelli, C.M., N. Bae, M. Almeida, D.T. Denhardt, C.E. Alpers, and S.M. Schwartz. 1993. Osteopontin is elevated during neointima formation in rat arteries and is a novel component of human atherosclerotic plaques. *J. Clin. Invest.* 92:1686–1696.
21. Giachelli, C.M., L. Liaw, C.E. Murry, S.M. Schwartz, and M. Almeida. 1995. Osteopontin expression in cardiovascular diseases. *Ann. N. Y. Acad. Sci.* 760:109–126.
22. O'Brien, E.R., M.R. Garvin, D.K. Stewart, T. Hinohara, J.B. Simpson, S.M. Schwartz, and C.M. Giachelli. 1994. Osteopontin is synthesized by macrophage, smooth muscle, and endothelial cells in primary and restenotic human coronary atherosclerotic plaques. *Arterioscler. Thromb.* 14:1648–1656.
23. Ikeda, T., T. Shirasawa, Y. Esaki, S. Yoshiki, and K. Hirokawa. 1993. Osteopontin mRNA is expressed by smooth muscle-derived foam cells in human atherosclerotic lesions of the aorta. *J. Clin. Invest.* 92:2814–2820.
24. Hirota, S., M. Imakita, K. Kohri, A. Ito, E. Morii, S. Adachi, H.M. Kim, Y. Kitamura, C. Yutani, and S. Nomura. 1993. Expression of osteopontin messenger RNA by macrophages in atherosclerotic plaques. A possible association with calcification. *Am. J. Pathol.* 143:1003–1008.
25. Fitzpatrick, L.A., A. Severson, W.D. Edwards, and R.T. Ingram. 1994. Diffuse calcification in human coronary arteries. Association of osteopontin with atherosclerosis. *J. Clin. Invest.* 94:1597–1604.
26. Takemoto, M., K. Yokote, M. Nishimura, T. Shigematsu, T. Hasegawa, S. Kon, T. Uede, T. Matsumoto, Y. Saito, and S. Mori. 2000. Enhanced expression of osteopontin in human diabetic artery and analysis of its functional role in accelerated atherogenesis. *Arterioscler. Thromb. Vasc. Biol.* 20:624–628.
27. Ahmed, S., K.D. O'Neill, A.F. Hood, A.P. Evan, and S.M. Moe. 2001. Calciphylaxis is associated with hyperphosphatemia and increased osteopontin expression by vascular smooth muscle cells. *Am. J. Kidney Dis.* 37:1267–1276.
28. O'Brien, K.D., J. Kuusisto, D.D. Reichenbach, M. Ferguson, C. Giachelli, C.E. Alpers, and C.M. Otto. 1995. Osteopontin is expressed in human aortic valvular lesions. *Circulation*. 92:2163–2168.
29. Shen, M., P. Marie, D. Farge, S. Carpentier, C. De Pollak, M. Hott, L. Chen, B. Martinet, and A. Carpentier. 1997. Osteopontin is associated with bioprosthetic heart valve calcification in humans. *C. R. Acad. Sci. III.* 320:49–57.
30. Srivatsa, S.S., P.J. Harrity, P.B. Maercklein, L. Kleppe, J. Veinot, W.D. Edwards, C.M. Johnson, and L.A. Fitzpatrick. 1997. Increased cellular expression of matrix proteins that regulate mineralization is associated with calcification of na-



- tive human and porcine xenograft bioprosthetic heart valves. *J. Clin. Invest.* 99:996–1009.
31. Canver, C.C., R.D. Gregory, S.D. Cooler, and M.C. Voytovich. 2000. Association of osteopontin with calcification in human mitral valves. *J. Cardiovasc. Surg. (Torino)*. 41:171–174.
  32. Giachelli, C.M., M. Scatena, and T. Wada. 1997. Osteopontin: potential roles in vascular function and dystrophic calcification. *J. Bone Miner. Metab.* 15:179–183.
  33. McKee, M.D., and A. Nanci. 1996. Osteopontin at mineralized tissue interfaces in bone, teeth, and osseointegrated implants: ultrastructural distribution and implications for mineralized tissue formation, turnover, and repair. *Microsc. Res. Tech.* 33:141–164.
  34. Wada, T., M.D. McKee, S. Steitz, and C.M. Giachelli. 1999. Calcification of vascular smooth muscle cell cultures: inhibition by osteopontin. *Circ. Res.* 84:166–178.
  35. Luo, G., P. Ducey, M.D. McKee, G.J. Pinero, E. Loyer, R.R. Behringer, and G. Karsenty. 1997. Spontaneous calcification of arteries and cartilage in mice lacking matrix GLA protein. *Nature*. 386:78–81.
  36. Liaw, L., D.E. Birk, C.B. Ballas, J.S. Whitsitt, J.M. Davidson, and B.L.M. Hogan. 1998. Altered wound healing in mice lacking a functional osteopontin gene (spp1). *J. Clin. Invest.* 101:1468–1478.
  37. Liaw, L., M. Almeida, C.E. Hart, S.M. Schwartz, and C.M. Giachelli. 1994. Osteopontin promotes vascular cell adhesion and spreading and is chemotactic for smooth muscle cells in vitro. *Circ. Res.* 74:214–224.
  38. Jono, S., M.D. McKee, C.E. Murry, A. Shioi, Y. Nishizawa, K. Mori, H. Morii, and C.M. Giachelli. 2000. Phosphate regulation of vascular smooth muscle cell calcification. *Circ. Res.* 87:e10–e17.
  39. Hildebrand, T., A. Laib, R. Muller, J. Dequeker, and P. Rueggsegger. 1999. Direct three-dimensional morphometric analysis of human cancellous bone: microstructural data from spine, femur, iliac crest, and calcaneus. *J. Bone Miner. Res.* 14:1167–1174.
  40. Steitz, S.A., M.Y. Speer, G. Curinga, H. Yang, P. Haynes, R. Aebersold, T. Schinke, G. Karsenty, and C.M. Giachelli. 2001. Smooth muscle cell phenotypic transition associated with calcification: upregulation of Cbfa1 and downregulation of smooth muscle lineage markers. *Circ. Res.* 89:1147–1154.
  41. Panda, D., G.C. Kundu, B.I. Lee, A. Peri, D. Fohl, I. Chackalaparampil, B.B. Mukherjee, X.D. Li, D.C. Mukherjee, S. Seides, et al. 1997. Potential roles of osteopontin and alphaVbeta3 integrin in the development of coronary artery restenosis after angioplasty. *Proc. Natl. Acad. Sci. USA*. 94:9308–9313.
  42. Otawara, Y., and P.A. Price. 1986. Developmental appearance of matrix GLA protein during calcification in the rat. *J. Biol. Chem.* 261:10828–10832.
  43. Romberg, R.W., P.G. Werness, B.L. Riggs, and K.G. Mann. 1986. Inhibition of hydroxyapatite crystal growth by bone-specific and other calcium-binding proteins. *Biochemistry*. 25:1176–1180.
  44. van de Loo, P.G., B.A. Soute, L.J. van Haarlem, and C. Vermeer. 1987. The effect of Gla-containing proteins on the precipitation of insoluble salts. *Biochem. Biophys. Res. Commun.* 142:113–119.
  45. Spronk, H.M., B.A. Soute, L.J. Schurgers, J.P. Cleutjens, H.H. Thijssen, J.G. De Mey, and C. Vermeer. 2001. Matrix Gla protein accumulates at the border of regions of calcification and normal tissue in the media of the arterial vessel wall. *Biochem. Biophys. Res. Commun.* 289:485–490.
  46. Engelse, M.A., J.M. Neele, A.L. Bronckers, H. Pannekoek, and C.J. de Vries. 2001. Vascular calcification: expression patterns of the osteoblast-specific gene core binding factor alpha-1 and the protective factor matrix gla protein in human atherogenesis. *Cardiovasc. Res.* 52:281–289.
  47. Price, P.A., G.R. Thomas, A.W. Pardini, W.F. Figueira, J.M. Caputo, and M.K. Williamson. 2001. Discovery of a high molecular weight complex of calcium, phosphate, ferritin, and matrix Gla protein in the serum of etidronate-treated rats. *J. Biol. Chem.* 277:3926–3934.
  48. Bostrom, K. 2001. Insights into the mechanism of vascular calcification. *Am. J. Cardiol.* 88:20E–22E.
  49. Doherty, T.M., and R.C. Detrano. 1994. Coronary arterial calcification as an active process: a new perspective on an old problem. *Calcif. Tissue Int.* 54:224–230.
  50. Bostrom, K., D. Tsao, S. Shen, Y. Wang, and L.L. Demer. 2001. Matrix GLA protein modulates differentiation induced by bone morphogenetic protein-2 in C3H10T1/2 cells. *J. Biol. Chem.* 276:14044–14052.
  51. Shanahan, C.M., N.R. Cary, J.R. Salisbury, D. Proudfoot, P.L. Weissberg, and M.E. Edmonds. 1999. Medial localization of mineralization-regulating proteins in association with Monckeberg's sclerosis: evidence for smooth muscle cell-mediated vascular calcification. *Circulation*. 100:2168–2176.
  52. Price, P.A., S.A. Faus, and M.K. Williamson. 1998. Warfarin causes rapid calcification of the elastic lamellae in rat arteries and heart valves. *Arterioscler. Thromb. Vasc. Biol.* 18:1400–1407.
  53. Hunter, G.K., C.L. Kyle, and H.A. Goldberg. 1994. Modulation of crystal formation by bone phosphoproteins: structural specificity of the osteopontin-mediated inhibition of hydroxyapatite formation. *Biochem. J.* 300:723–728.
  54. Jono, S., C. Peinado, and C.M. Giachelli. 2000. Phosphorylation of osteopontin is required for inhibition of vascular smooth muscle cell calcification. *J. Biol. Chem.* 275:20197–20203.
  55. Tintut, Y., F. Parhami, K. Bostrom, S.M. Jackson, and L.L. Demer. 1998. cAMP stimulates osteoblast-like differentiation of calcifying vascular cells. Potential signaling pathway for vascular calcification. *J. Biol. Chem.* 273:7547–7553.
  56. Shioi, A., Y. Nishizawa, S. Jono, H. Koyama, M. Hosoi, and H. Morii. 1995. Beta-glycerophosphate accelerates calcification in cultured bovine vascular smooth muscle cells. *Arterioscler. Thromb. Vasc. Biol.* 15:2003–2009.
  57. Watson, K.E., K. Bostrom, R. Ravindranath, T. Lam, B. Norton, and L.L. Demer. 1994. TGF-beta 1 and 25-hydroxycholesterol stimulate osteoblast-like vascular cells to calcify. *J. Clin. Invest.* 93:2106–2113.